SLAC–PUB–9808
May 2003

Use of Acoustic Emission to Diagnose Breakdown in Accelerator RF Structures [*]

J. Nelson, M. Ross, J. Frisch, F. Le Pimpec, K. Jobe, D. McCormick, T. Smith
Stanford Linear Accelerator Center, Stanford University, Stanford CA 94309

Abstract

Accelerator structures of a wide variety have been damaged by RF breakdowns. Very little is known about the mechanisms that cause the breakdown and the damage although there has been theoretical work [1,2]. Using an array of ultrasonic acoustic emission sensors we have been able to locate and classify breakdown events more accurately than possible using microwave techniques. Data from the technique has led to improvements in the design of the NLC X-band RF structure. We report results of acoustic emission studies at the DESY TESLA Test Facility and the SLAC NLC Test Accelerator.

Contributed to Particle Accelerator Conference 2003

Portland, Ore., 12-16 May 2003

[*] Work supported by Department of Energy contract DE–AC03–76SF00515.

Abstract

Accelerator structures of a wide variety have been damaged by RF breakdowns. Very little is known about the mechanisms that cause the breakdown and the damage although there has been theoretical work [1,2]. Using an array of ultrasonic acoustic emission sensors we have been able to locate and classify breakdown events more accurately than possible using microwave techniques. Data from the technique has led to improvements in the design of the NLC X-band RF structure. We report results of acoustic emission studies at the DESY TESLA Test Facility and the SLAC NLC Test Accelerator.

INTRODUCTION

The Next Linear Collider (NLC) project requires X-band copper structures capable of operating at accelerating gradients of about 70 MV/m with a breakdown rate less than 0.1/hour. To understand the higher breakdown rates seen, a tool is needed that is able to localize the deposited energy within a few square mm around the iris.

In [1] a breakdown mechanism is proposed which entails a small plasma spot forming near an iris. This model predicts surface melting in the region of the plasma spot as well as energy deposition on an opposing iris. If so, a tool capable of localizing the breakdown should be able to distinguish this phenomenon from a breakdown affecting only one iris.

Acoustic emission sensors (AES) were used to localize breakdowns in multiple scenarios: L-band RF gun and X-band accelerating structures, as well as studying breakdown patterns associated with X-band structure processing.

ACOUSTIC EMISSION SENSORS

Acoustic emission sensors are piezo-electric devices used in industrial non-destructive testing of such things as crack propagation in airplane frames. In the X-band case, heat from the 40 joule RF pulse is absorbed in the structure walls causing thermal expansion which creates sound that we can detect in the 100 kHz – 1 MHz range. We see little attenuation at these frequencies; however, at higher frequencies the attenuation is strongly dependent on crystalline structure. While we don't have an absolute calibration of the amplitude of the vibrations in the copper, one can readily hear breakdowns and even normal events in the structure.

Acoustic waves propagate in annealed copper as bulk shear (*s*) waves with a speed v_s = 2325 m/s, bulk pressure (*p*) waves, v_b = 4760 m/s, or as a slower shear wave [3]. At our detectable frequencies, the shear wave disturbance wavelength is about 10 mm, the characteristic dimension of X-band RF cell widths, but significantly smaller than L-band components.

DATA

L-Band

The TESLA Test Facility (TTF) normal-conducting L-band 1.5 cell RF photocathode gun has exhibited breakdown activity near its peak design power and pulse length [4]. The determination of the breakdown location is more easily done with acoustic sensors than with standing wave microwave localization techniques.

Eight sensors were attached to the copper gun cavity and waveguide with cyano-acrylate glue. The sensors' signals were locally amplified then recorded with oscilloscopes outside the tunnel housing. Figure 1 below shows sensor signals from a typical breakdown event. The breakdown signals are up to 100 times larger than the signals produced on a non-breakdown pulse.

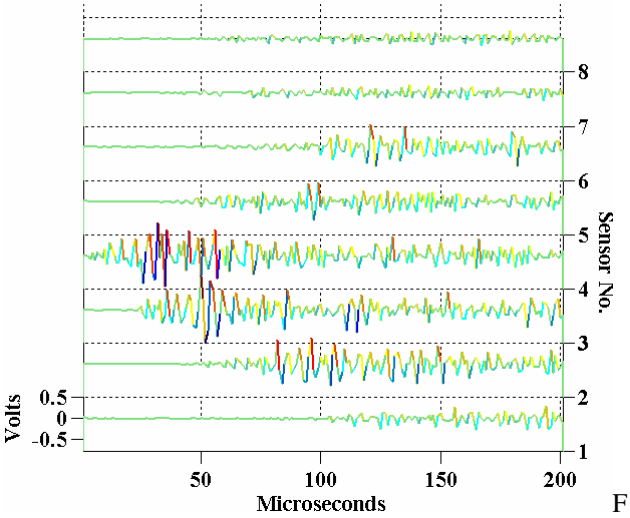

Figure 1: Recorded voltage signals from TTF gun acoustic sensors from a single breakdown event.

In Fig. 1, the breakdown signals that are largest and arrive earliest (sensors 3 and 4) are around the waveguide coupler iris. Those that are small and arrive later (sensors 7 and 8) are attached to the gun's cavity coupler cell and close to the cathode, respectively. The shapes of the envelopes of the signals are not understood.

X-Band

At the NLC Test Accelerator (NLCTA) an aggressive structure testing program is underway to refine structure designs to achieve the NLC required parameters. The structures' achievable gradients are limited by breakdowns and ultimately by the damage they cause [5]. To diagnose this problem, 64 sensors are attached to a copper X-band accelerating structure, typically glued 4

sensors per structure cell, 90 degrees apart. The signals are digitized at 10 MHz. Each waveform contains 100 μs of a sensor's signals from three consecutive RF pulses with the last pulse being the breakdown pulse.

Figure 2 shows two consecutive pulses for 12 sensors (3 cells, 4 sensors per cell). Sensor 6 shows the largest signal, about 30 times larger than the non-breakdown pulse. Adjacent sensors 2 and 10 have relatively small signals, indicating very localized energy deposition at sensor 6.

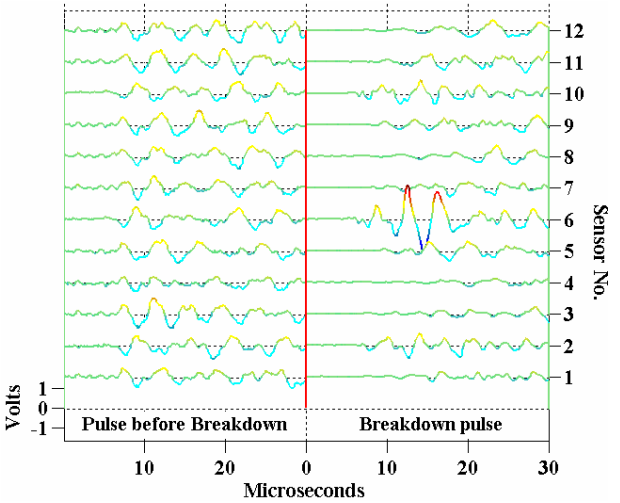

Figure 2: Two consecutive RF pulses in NLCTA. The amplitude of the non-breakdown pulse has been increased 10x.

ANALYSIS

Breakdown localization

We determine breakdown location using two methods: (1) time of arrival t_0 of the breakdown signal at the sensor and (2) relative amplitude of the sensor signals σ_{norm}.

To identify the time of arrival of the breakdown signal at a given sensor, we first calculate the integrated rms of each sensor's signal,

$$R_n(t) = \sigma_n[V_n(1,2,\ldots t)], \qquad (1)$$

where t is time in 0.1 μs data points, V is the acoustic sensor signal voltage, σ is the rms, and R is the integrated rms from 1 to t. The subscript n denotes the breakdown pulse; subscript n-2 denotes the non-breakdown pulse 2 pulses before.

At TTF, the time of arrival was determined as when the integrated rms crossed a threshold, R_0:

$$t_0=t \text{ when } R(t)>R_0. \qquad (2)$$

For NLCTA, we used:

$$t_0=t \text{ when } [R_n(t)/R_{n-2}(t)]>R_0. \qquad (3)$$

At TTF the division by R_{n-2} wasn't necessary as the acoustic signals on non-breakdown pulses were so small.

Another way to determine breakdown location is to look at the relative amplitude of the signals seen at the sensors:

$$\sigma_{norm}=R_n(20\mu s)/R_{n-2}(20\mu s). \qquad (4)$$

RESULTS

Particle Contamination in X-band Structures

For one of the NLC test structures, a week's worth of processing, 2366 breakdowns, was analyzed using the σ_{norm} technique. It was discovered that more than 600 breakdowns occurred in one location – the twelfth cell of the structure, a rate six times more than the typical cell average. Of the events in cell 12, 83% showed the highest signal from the sensor on the bottom of the cell. Based on the AES data, the structure was dissected at that cell. We found a 0.5mm by 1mm sliver of aluminum near the location of the largest σ_{norm}. The particle was surrounded by many craters and melted spots.

X-band Structure Input Coupler

AES gave conclusive evidence of breakdown in the low electric field region of the input coupler. This unexpected result prompted the redesign of the coupler to reduce pulse heating (possibly due to high magnetic fields) on the four input waveguide matching irises. This work is summarized in [6,7].

TTF

For the TTF L-band gun the breakdowns were isolated to the input waveguide coupling iris, not the cathode as originally suspected. Typical signals from the 3 sensors on this iris are shown in figure 1 as signals 3, 4, and 5. Using the t_0 technique and given the distance between the sensors and the potential breakdown sources, one can pinpoint the breakdown location between sensors 4 and 5, as well as calculate the speed of the signal's propagation: 3520 ± 810 m/s. This speed is between the p and s wave speeds. The sensors probably see both waves with differing sensitivities.

Multiple-Iris Events in X-band Structures

Given a data set of a few thousand breakdowns for a particular structure from a month's running, we chose to select just the events which appear to be highly localized, namely those meeting the following criteria: for a given sensor, i, and its axial neighbors, i±1,

$$\sigma_{norm}(i)>20 \quad \text{and} \quad \sigma_{norm}(i\pm1)< \sigma_{norm}(i)/2.$$

This selected 15 of the 400 events in the body of the structure. Figure 3 shows a typical event of this type.

This figure shows that the sensors' resolution is less than the distance between the sensors around the cell and about equal to the cell spacing. Using the t_0 technique, we found that the signals from sensors i±1 arrive at the same time, approximately 1 μs later than the signal from

sensor *i*. Given that the sensors are mounted between the irises, the breakdown can only be coming from both irises, not just one. This result is consistent with the theory proposed in [1,2].

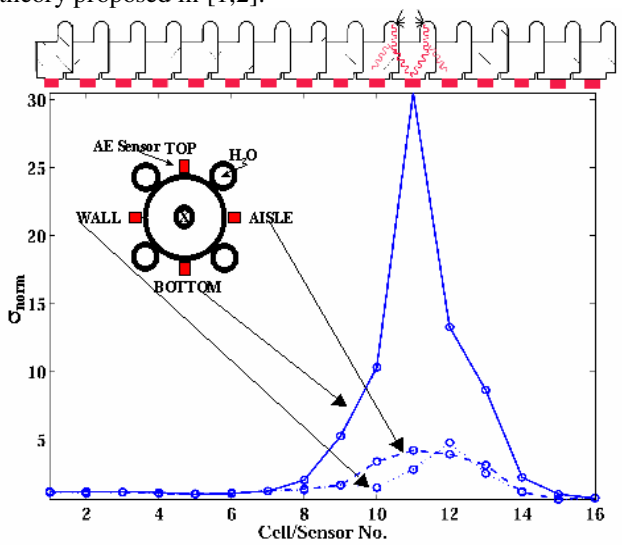

Figure 3: σ_{norm} for a typical multiple-iris event. The solid line connects data from 16 sensors, one per cell, in a row. Along the top is a schematic of the structure, showing the placement of the sensors between the irises as well as a possible path for the sound from the breakdown to travel. The inset shows the sensors mounted around a cell. Of note is the vertical scale: more than 30 times the energy deposited on a non-breakdown pulse is seen by one sensor.

Spitfests in X-band Structures

Another phenomenon seen during processing of the X-band structures in NLCTA is the so-called spitfest –when breakdowns are rare, but clustered in time. For example, there will be no breakdowns for more than 30 minutes, followed by many breakdowns in quick succession, less than two minutes apart. Some of these breakdowns occur at very low voltage. From a two week, steady-state running period with 288 breakdowns, 141 happened within two minutes of the previous event in 62 spitfest groups. Figure 4 below shows the locations of seven breakdowns that happened in one spitfest sequence.

This figure shows that subsequent breakdowns aren't confined to the same location as the first breakdown and actually vary their locations by more than just a few cells. This is inconsistent with the assumption that subsequent breakdowns happen near the surface damage caused by the first breakdown.

CONCLUSIONS

AES have proven uniquely suited to locating breakdowns in RF components. Two analysis techniques provide complementary information: relative signal power and signal timing. Using these two techniques, we have been able to diagnose many problems including particle contamination and high pulse heating regions as well as better understand the multiple-iris breakdown process in X-band structures and the spitfest phenomenon seen during processing.

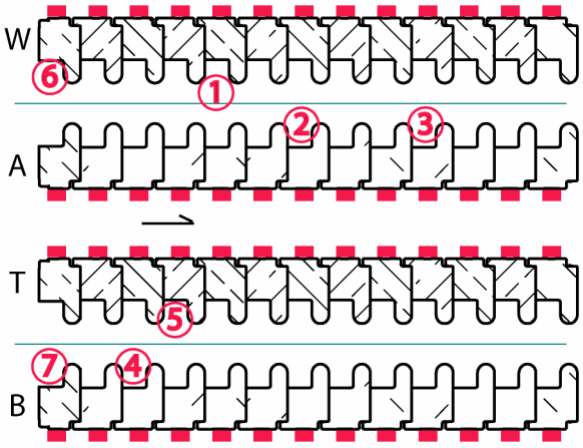

Figure 4: Sketch of a section of a 60-cell X-band structure showing the location of a series of breakdowns in a spitfest. The rows correspond to the rows of sensors on the structure: on the wall, aisle, top and bottom sides.

FUTURE PLANS

Future plans include adding another 80 sensors to give a total of 144. This should help better understand events with multiple breakdowns on one pulse. AES will also be used to diagnose breakdowns in high power components of the 8-pack RF distribution system installation.

ACKNOWLEDGEMENTS

The authors thank R. Kirby and S. Harvey for the structure autopsies and acknowledge K. Ratcliffe's many contributions to the NLCTA structure program.

REFERENCES

[1] P. Wilson, "Frequency and Pulse Length Scaling of RF Breakdown in Accelerator Structure," (2001) SLAC-PUB-9114.

[2] P. Wilson, "Gradient Limitation in Accelerating Structures Imposed by Surface Melting," TPAB039, this conference.

[3] J. Nelson and M. Ross, "Studies of TTF RF Photocathode Gun using Acoustic Sensors," (2001) SLAC-PUB-9340.

[4] S. Schreiber, et. al., "First Experiments with the RF Gun Based Injector for the TESLA Test Facility Linac," PAC'99, March 1999, New York, NY.

[5] C. Adolphsen, "Normal-Conducting RF Structure Test Facilities and Results," ROPC006, this conference.

[6] J. Frisch, et. al. “Studies of Breakdown in High Gradient X-Band Accelerator Structures using Acoustic Emission,” (2002) SLAC-PUB-9469.
[7] V. Dolgashev, “Experiments on Gradient Limits for Normal Conducting Accelerators,” LINAC 2002, August 2002, Gyeongju, Korea.